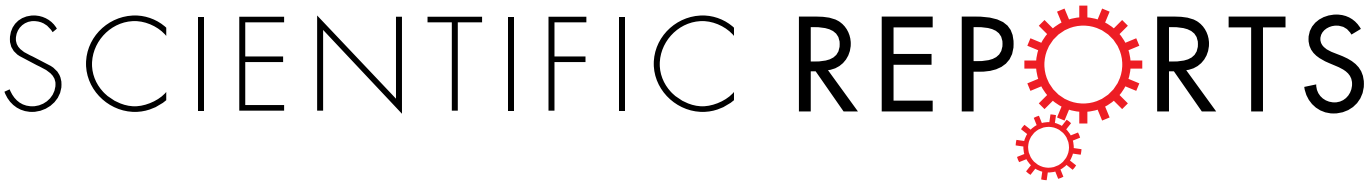

OPEN

# Design of a Yellow-Emitting Phosphor with Enhanced Red Emission via Valence State-control for Warm White LEDs Application

Received: 12 April 2016
Accepted: 14 July 2016
Published: 11 August 2016

Jian Chen[1], Yangai Liu[1], Lefu Mei[1], Peng Peng[2], Qijin Cheng[3] & Haikun Liu[1]

**The phosphor-converted warm W-LED have being rapidly developed due to the stringent requirements of general illumination. Here, we utilized a strategy to synergistically enhance the red region and emission intensity of novel Eu-activated yellow-emitting $LaSiO_2N$ phosphors. This was realized by predicting optimum crystal structure, and governing the concentration of doping ions as well as preparation temperature. By using these straight-forward methods, we were able to vary the valence to enhance the red region and improve the quantum efficiency of $LaSiO_2N$ phosphor. The warm W-LED lamp fabricated with this red region enhanced $LaSiO_2N$:Eu phosphor exhibited high CRI (Ra = 86), suitable CCT (5783 K) and CIE chromaticity (0.33, 0.36), indicating this synergistically enhanced strategy could be used for design of yellow-emitting phosphor materials to obtain warm W-LEDs.**

Due to the deficiency of red color, the cool and bluish-white light LEDs (typically a blue-light LED chip coupled with yellow-emitting YAG: $Ce^{3+}$ phosphor) with high correlated color temperature (CCT) and low color rendering index (CRI) are gradually replaced by blue, green and red (RGB)-emitting phosphors with a UV/NUV chip[1,2]. However, high cost and poor luminous efficiency of RGB-emitting phosphor became the main obstacles of their popularization because of self-adsorption occurring among these phosphor particles[3]. Currently, the white LEDs (W-LED) packaged by NUV chips (365–420 nm) with mixed blue and yellow-red emitting phosphors have attracted much attention because of their high CRI, tunable CCT and CIE chromaticity coordinates[4–11]. Therefore, designing and developing tunable yellow-red emitting phosphors which can be effectively excited with NUV light are in great demand for W-LED industry.

Currently, La–Si–O–N system doped with $Ce^{3+}$ ions has been widely reported as blue phosphors for the application in solid-state lighting, fluorescent lamps or plasma display panels (PDPs)[12,13]. The emission properties of this La–Si–O–N system doped with $Ce^{3+}$ or $Eu^{2+}$ strongly depend on Si/La and N/O ratios, because the 5*d* electrons of $Ce^{3+}$ and $Eu^{2+}$ ions are unprotected and sensitive to the change of the strength of crystal field and covalency[14,15]. According to the crystallographic examination for an equal amount of $Ce^{3+}$ substitution, the degree of covalency increased in a sequence of $La_5Si_3O_{12}N < La_4Si_2O_7N_2 < La_2Si_6O_3N_8 < LaSiO_2N$[16]. As supported by Dorenbos[17], the emission position depended on nephelauxetic effect, crystal-field splitting (CFS), and Stokes shift. Herein, $Eu^{2+}$ ions in $LaSiO_2N$ should have stronger nephelauxetic effect due to its high covalency, compared with other La–Si–O–N system compounds. This effect would shift the centroid of the 5*d* band of $Eu^{2+}$ ions to lower energy and result in the redshift of emission peak. Meanwhile, the higher formal charge of $N^{3-}$ compared with $O^{2-}$ makes the CFS become larger, and the rigid lattice would lead to a smaller Stokes shift[18]. Thus, the $LaSiO_2N$ doped with lanthanide, especially $Eu^{2+}$, may emit long-wave bands. But until now, the $Eu^{2+}$ photoluminescence in La–Si–O–N system has been rarely reported due to the charge mismatch of $Eu^{2+}$ and $La^{3+}$. However, in our recent experiment, we observed the $Eu^{2+}$ photoluminescence in $LaSiO_2N$, and this novel $LaSiO_2N$: Eu phosphor, as expected, exhibited broad emitting in yellow region. Further, we designed a strategy to cooperatively enhance the red region and emission intensity of this phosphor via altering the concentration of doping ions and preparation temperature for high CRI warm W-LED application. The red region enhancements were caused by

[1]Beijing Key Laboratory of Materials Utilization of Nonmetallic Minerals and Solid Wastes, National Laboratory of Mineral Materials, School of Materials Science and Technology, China University of Geosciences, Beijing 100083, china. [2]Department of Materials Processing and Control Engineering, School of Mechanical Engineering and Automation, Beihang University, Beijing, 100191, China. [3]School of Energy Research, Xiamen University, Xiamen 361005, Fujian, China. Correspondence and requests for materials should be addressed to Y.L. (email: liuyang@cugb.edu.cn)

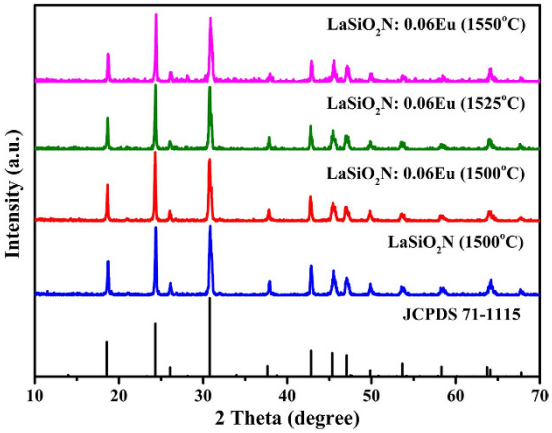


**Figure 1. XRD patterns of as-synthesized $LaSiO_2N$:Eu phosphors, $LaSiO_2N$ host and the standard pattern (JCPDS 71–1115) of $LaSiO_2N$.**

varied valence which would affect the energy level of 5*d* band of $Eu^{2+}$ and charge-transfer state of $Eu^{3+}$, resulting in redshift and the increase of absorption efficiency as well as energy transfer from $Eu^{2+}$ to $Eu^{3+}$. Fabricated by using a blend of $LaSiO_2N$: Eu and commercial blue phosphors (BAM: $Eu^{2+}$) with a 385 nm NUV LED chip, a warm white light with high CRI as well as suitable CCT and CIE chromaticity can be obtained.

## Results and Discussion

The phase purity of the as-prepared $LaSiO_2N$:Eu phosphors and $LaSiO_2N$ host were substantiated by powder X-ray diffraction. As the Fig. 1 illustrated, all the diffraction peaks matched well with the standard pattern (JCPDS 71–1115) of $LaSiO_2N$, demonstrating that the doping of Eu ions and the increased preparation temperature did not significantly influence its crystal structure.

Figure 2a presents the crystal structure, photoluminescence excitation (PLE) and photoluminescence (PL) spectra of the $LaSiO_2N$:0.01Eu phosphor prepared at 1500 °C. The $LaSiO_2N$ crystallizes as a hexagonal structure whose space group is P-6c2, and lattice constants are a = 7.31 Å, c = 9.550 Å, and V = 441.95 $Å^3$. $LaSiO_2N$ has the α-wollastonite structure with N atoms present in the three-membered ($Si_3O_6N_3$) rings, occupying bridging sites between pairs of Si-centered tetrahedral and linking to two La atoms[19]. Hence, the N environment is more ionic, and the lattice is more rigid than that of $Si_3N_4$ or $Si_2N_2O$. Based on the crystal structure, the $LaSiO_2N$:Eu phosphor could be predicted to emit broad and long-wave band, and the following studies would verify this inference.

As shown in Fig. 2a, The PLE spectrum of $LaSiO_2N$:0.01Eu monitored by 554 nm was composed of a broad excitation peaked at 365 nm ranging from 250–500 nm, which can be attributed to the $4f^7(^8S7/2)$–$4f^65d^1$ transition of $Eu^{2+}$ ions[20], and matched well with the emission of commercial N-UV chip (365–420 nm). The reduction of $Eu^{3+}$ to $Eu^{2+}$ in the trivalent La site can be explained with the charge compensating defect in the first anion ($O^{2-}$ ion) coordination shell[17]. The PL spectrum of $LaSiO_2N$:0.01Eu under 365 nm light excitation exhibited a broad yellow band from 450 to 750 nm peaked at 554 nm with a full width at half-maximum (FWHM) of 115.87 nm which was larger than that of YAG phosphor (91.65 nm), indicating that the synthesized phosphor here is a suitable yellow-emitting phosphor candidate for W-LED application.

Figure 2b depicts the Eu concentration dependent PL spectra of $LaSiO_2N$:*x*Eu (*x* = 0.01, 0.02, 0.04, 0.06, 0.08) phosphors with a 365 nm excitation. It is noteworthy that the shoulder peaks at 596 nm, 614 nm and 660 nm arose increasingly along with the increased Eu concentration. These shoulder peaks is reasonable to attribute to the unreduced $Eu^{3+}$ ions and can be assigned to 4f-4f transitions of $Eu^{3+}$ ($^5D_0$-$^7F_J$ (J = 1, 2 and 3))[21]. As the doping concentration of Eu increased to 6 mol%, the emission intensity reached the maximum and then declined dramatically with a further increase of concentration. Generally, the declined intensity with increased concentration is caused by the concentration quenching effect[22]. Such effect is mainly caused by the energy consumption via energy transfer from one activator to another[23]. When the concentration of Eu increased gradually, the interatomic distance between the two Eu ions reduced, and the energy transfer rate between $Eu^{2+}$-$Eu^{2+}$ as well as the probability of energy transfer to luminescent killer sites increased[24]. Simultaneously, the interaction was more intensive with the reduction of interatomic distance. As a result, the *5d* band of $Eu^{2+}$ ion decreased and led to the redshift of emission peak[25]. As depicted in Fig. 2b, an obvious redshift of emission peak occurred, indicating the intensive interaction between the identical activators[26]. However, as shown in Fig. 3, the decay curves of $LaSiO_2N$:*x*Eu (*x* = 0.01–0.08) monitored at 565 nm obviously consist of two lifetimes and all decay curves could be well fitted via the second-order exponential equation[27]:

$$I(t) = A_1 \exp(-t/\tau_1) + A_2(-t/\tau_2) \quad (1)$$

where *I* means the luminescence intensity; $A_1$ and $A_2$ are constants; *t* is time; and $\tau_1$ and $\tau_2$ are the lifetimes for the exponential components. As previous researches report that there is only one single La site can be substituted by Eu ion[14,16]. Thus, the existence of two lifetimes may due to the two kinds of decay forms for Eu:$^{2+}$ one is the process of electrons from the excited stated to ground state; the other is the energy transfer process between $Eu^{2+}$

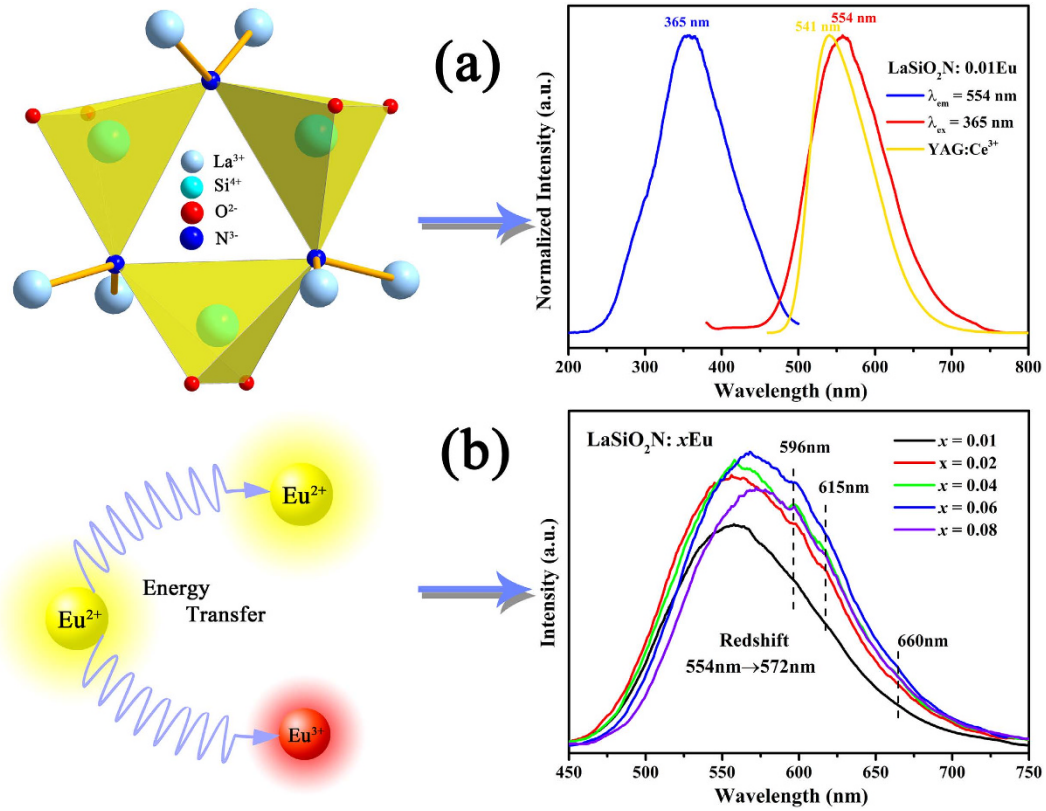


**Figure 2.** (**a**) Crystal structure, PLE ($\lambda_{em} = 554$ nm) and PL ($\lambda_{ex} = 365$ nm) spectra of the $LaSiO_2N$:0.01Eu phosphor (prepared at 1500 °C); (**b**) Eu concentration-dependent PL ($\lambda_{ex} = 365$ nm) spectra of $LaSiO_2N$:*x*Eu ($x = 0.01, 0.02, 0.04, 0.06, 0.08$) phosphors (prepared at 1500 °C), and the corresponding schematic illustration.

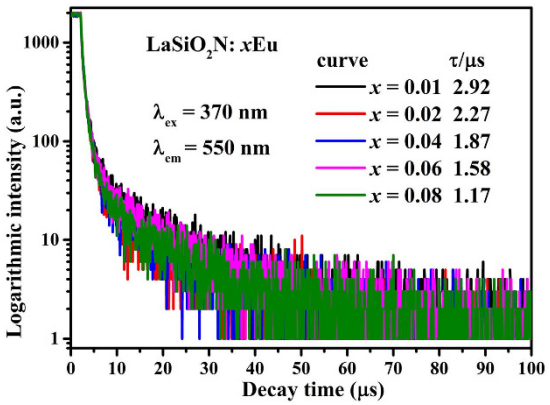


**Figure 3. The decay curves of $LaSiO_2N$:*x*Eu ($x = 0.01, 0.02, 0.04, 0.06, 0.08$).**

and $Eu^{3+}$ because of the coexisting of $Eu^{2+}$ and $Eu^{3+}$. The average lifetime $\tau^*$ could be reckoned according to the following equation:

$$\tau^* = (A_1\tau_1^2 + A_2\tau_2^2)/(A_1\tau_1 + A_2\tau_2) \quad (2)$$

based on eqs 1 and 2, the $\tau^*$ can be estimated to 2.92, 2.27, 1.87, 1.58, and 1.17 μs for $LaSiO_2N$:*x*Eu with $x = 0.01$, 0.02, 0.04, 0.06 and 0.08, respectively. The donor decay times decreased as Eu concentrations increased, indicating the existence of energy transfer processes[28,29]. Therefore, the phenomenon of declined intensity in $LaSiO_2N$:Eu might both result from the energy transfer between $Eu^{2+}$-$Eu^{2+}$ and $Eu^{2+}$-$Eu^{3+}$.

The excitation spectra of $LaSiO_2N$:0.06Eu were shown in Fig. 4a. Although the excitation band of $Eu^{3+}$ were covered by that of $Eu^{2+}$, the charge-transfer state (CTS) could be identified from the excitation spectra of $LaSiO_2N$:0.06Eu under different emission features at 565 nm, 596 nm, 615 nm and 660 nm. The relative intensity

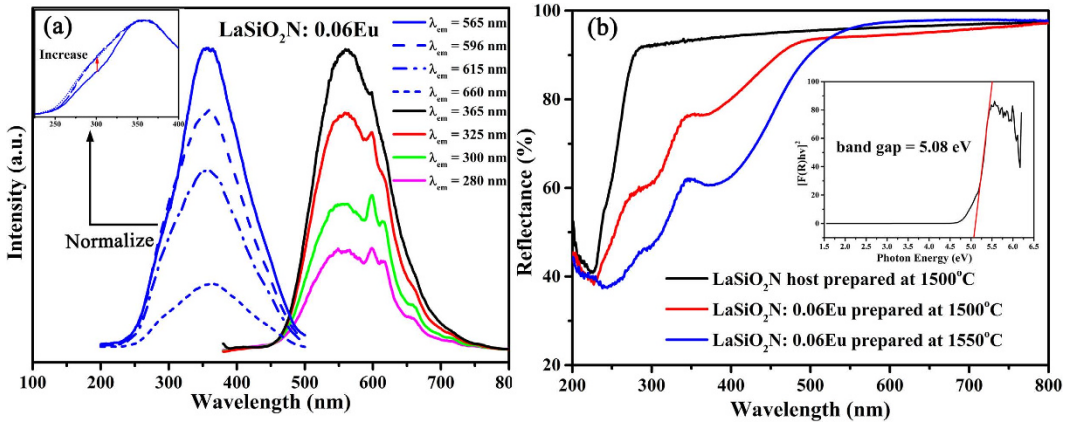


**Figure 4.** (**a**) PLE and PL spectra of the $LaSiO_2N$:0.06Eu phosphor monitored by different wavelengths of emission and excitation, respectively; (**b**) Diffuse reflection spectra of $LaSiO_2N$ host and $LaSiO_2N$:0.06Eu (prepared at 1500 °C and 1550 °C). The inset shows the absorption spectrum of $LaSiO_2N$ host calculated using the Kubelka-Munk equation.

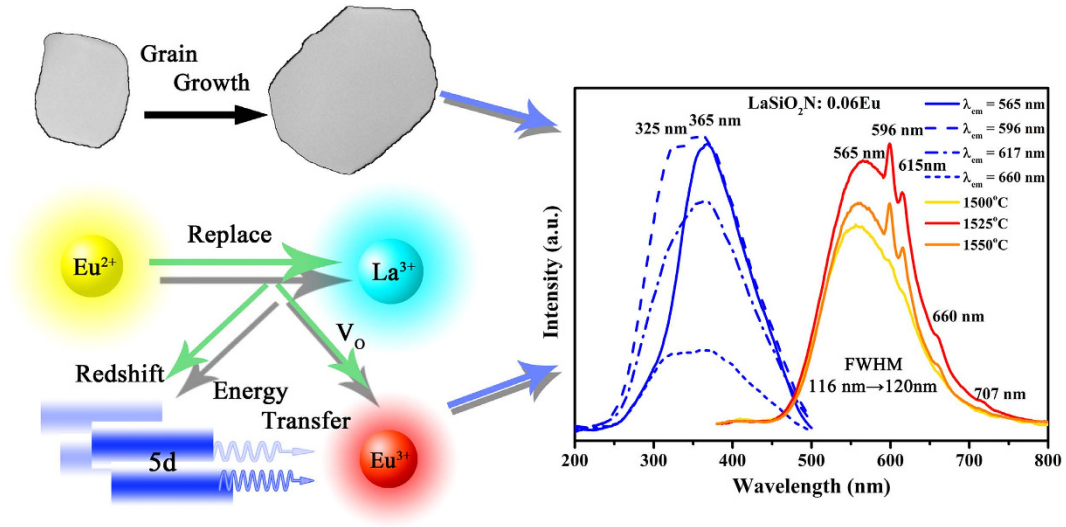


**Figure 5. The schematic illustration of the mechanism of red enhanced Yellow-emitting $LaSiO_2N$:Eu phosphor.** PLE ($\lambda_{em}$ = 565 nm, 596 nm, 617 nm, 660 nm ) spectra of the $LaSiO_2N$:0.06Eu phosphors (prepared at 1550 °C), and PL ($\lambda_{ex}$ = 365 nm) spectra of the $LaSiO_2N$:0.06Eu phosphors as a function of the preparation temperature (1500 °C, 1525 °C, and 1550 °C).

of shoulder peak at around 300 nm increased from 565 nm to 660 nm excitation, suggesting it played a key role in generation of the $Eu^{3+}$ emission. Theoretically, charge-transfer state (CTS) or the energy transfer from host lattice (HL) to $Eu^{3+}$ can generate this shoulder peak[25]. For detailed investigation of the source of the shoulder peak, the diffuse reflectance spectra (DRS) of $LaSiO_2N$ host and $LaSiO_2N$:0.06Eu were presented in Fig. 4b. The $LaSiO_2N$ host showed an energy absorption in the short-wavelength UV region (peaked at 225 nm) and a high reflection ranging from 275 to 800 nm. The band gap was estimated to be about 5.08 eV (244 nm) based on the Kubelka-Munk function[30]. When Eu ions were introduced into the $LaSiO_2N$ host, two broad absorption bands were observed in the 275–350 nm and 350–500 nm, demonstrating that the shoulder peak unlikely originated from HL. The emission spectra of $LaSiO_2N$:0.06Eu under different excitations were also illustrated in Fig. 4a. Each emission spectrum was consist of luminescence characteristics of both $Eu^{2+}$ and $Eu^{3+}$ ions, and the relative intensity of $Eu^{3+}$ reached the maximum at 300 nm, further proving the shoulder peak at 300 nm is assigned from CTS. It suggests that the coexistence of $Eu^{3+}$ and $Eu^{2+}$ can be realized to enhance the red region, while the emission efficiency of $Eu^{3+}$ is insufficient to generate a marked effect.

For further improving the red region of $LaSiO_2N$:Eu phosphor, the preparation temperature was changed, and all temperatures were controlled in the range from 1500 °C to 1550 °C to insure the obtained samples are single phase. Figure 5 shows the room temperature PLE ($\lambda_{em}$ = 565 nm, 596 nm, 617 nm, and 660 nm) of the $LaSiO_2N$:0.06Eu phosphors prepared at 1550 °C, and PL ($\lambda_{ex}$ = 365 nm) spectra of the $LaSiO_2N$:0.06Eu phosphors as a function of the preparation temperature (1500 °C, 1525 °C, and 1550 °C). The enlargement of shoulder peak

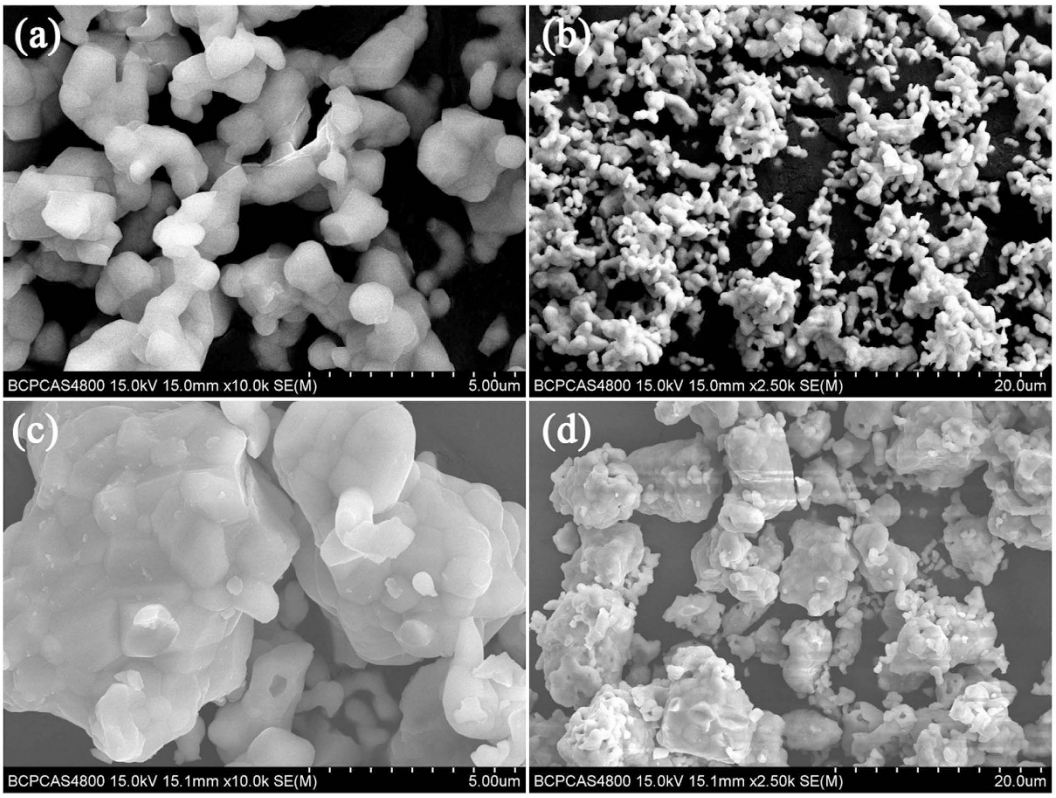


**Figure 6.** SEM images of the $LaSiO_2N$:0.06Eu phosphors prepared at (**a,b**) 1500 °C and (**c,d**) 1550 °C.

(325 nm) from $Eu^{2+}$ emission feature excitation to that of $Eu^{3+}$ also proved the shoulder peak derived from CTS. It is interesting that not only all the emission intensities were enhanced through the increase of the preparation temperature, but also the relative intensity of $Eu^{3+}$ characteristic peak was enhanced compared with that of $Eu^{2+}$. One of reason for the increase of holistic emission intensity may be due to grain growth and the increased degree of crystallization at a higher preparation temperature[31,32]. It can be substantiated by the micro-morphology of the crystalline $LaSiO_2N$:0.06Eu phosphors which were observed via SEM, TEM and XRD Refinement. As depicted in Fig. 6, the particles prepared at 1500 °C (Fig. 6a,b) had irregular morphology with the diameters ranging from 0.3 to 0.8 μm. When the preparation temperature increased, the edges and corners of irregular particles became clear, and a dramatic increase in particle sizes was observed (Fig. 6c,d). In addition, a mass of primary crystals reunited to be particles, and the obvious "sintering necks" between primary crystals suggested that grain growth occurred during the process of synthesis. The typical TEM images were illustrated in Figure S1 to further prove the grain growth. After Jade software refined, the relative crystallinity of $LaSiO_2N$:0.06Eu prepared at 1500 °C and 1550 °C were estimated about 82.38% and 89.91%, respectively, demonstrating the increased degree of crystallization at a higher preparation temperature.

To compare the ratio changing of $Eu^{2+}$ and $Eu^{3+}$, the high-resolution XPS spectra at the Eu 3d of $LaSiO_2N$:0.06Eu phosphors prepared at 1500 °C, 1525 °C, and 1550 °C were detected, respectively. As exhibited in Fig. 7, two peaks were found at around 1128 eV and 1135 eV, and the shapes as well as binding energies of the Eu3d signals in $LaSiO_2N$:0.06Eu agreed well with the signals of $Eu^{2+}$ $3d_{5/2}$ and $Eu^{3+}$ $3d_{5/2}$, respectively, indicating the existence of $Eu^{2+}$ and $Eu^{3+}$ ions[33]. Additionally, the relative intensity of $Eu^{3+}$ $3d_{5/2}$ signals was gradually decreased with the increased preparation temperature, revealing the promotion of reduction process of $Eu^{3+}$. This may due to the amount of thermal defects increased with the increasing preparation temperatures[34,35], which could charge compensate the $Eu^{2+}$ in the $La^{3+}$ site and improved the reduction from $Eu^{3+}$ to $Eu^{2+}$ [17]. Thus, the increase of $Eu^{2+}$ concentration may be a reason for the enhanced emission intensity of $Eu^{2+}$. However, decreased ratio of $Eu^{3+}$ concentration compared with $Eu^{2+}$ was inconsistent with the enhanced emission intensity of $Eu^{3+}$. Hence, other assistance might be involved to contribute the characteristic emissions of $Eu^{3+}$ in $LaSiO_2N$.

As illustrated in Fig. 8, the PLE ($\lambda_{em} = 596$ nm) spectra of the $LaSiO_2N$:0.06Eu phosphors prepared at 1500 °C, 1525 °C, and 1550 °C were deconvoluted into three Gaussian components, respectively. The relative intensity of CTS (fit peak 3) was enhanced, indicating that the charge transfer from the $O^{2-}$ to $Eu^{3+}$ was enhanced and more efficient with the increasing preparation temperatures. This phenomenon can be explained based on the increase of oxygen vacancies ($V_o$) with the increase of nonequivalent substitution of $La^{3+}$ by $Eu^{2+}$ in the host[25]. These $V_o$ might act as sensitizers for the energy transfer from host to $Eu^{3+}$ ion due to the strong mixing of charge transfer states[36–39]. Thus, the relative emission of $Eu^{3+}$ was enhanced, and the red region of this yellow emitting phosphor was promoted. Meanwhile, an obviously redshift of CTS occurred as the preparation temperature increased, which can be attributed to the increase of $Eu^{3+}$-$O^{2-}$ bond length. Since the $Eu^{2+}$ ions have smaller

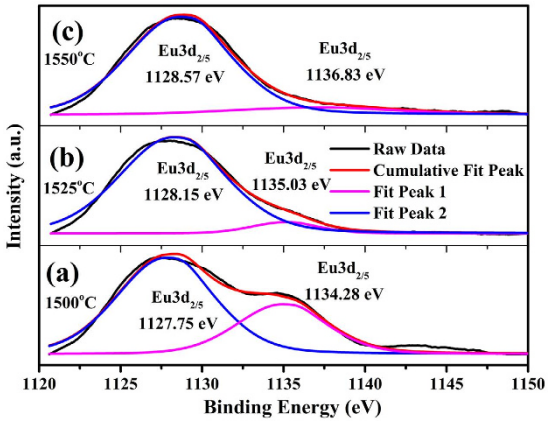


**Figure 7.** High-resolution XPS spectra at Eu 3d position of $LaSiO_2N$:0.06Eu phosphors prepared at (**a**) 1500 °C, (**b**) 1525 °C and (**c**) 1550 °C.

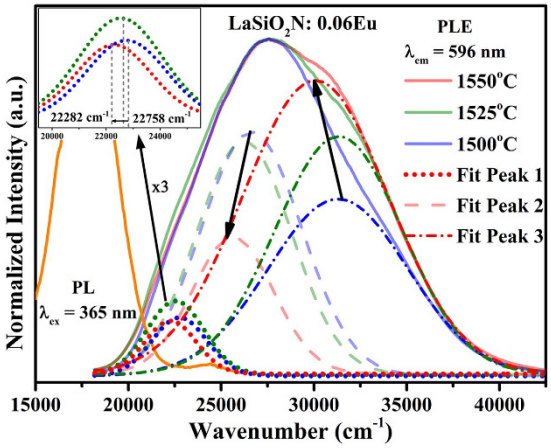


**Figure 8. Normalized PLE spectra ($\lambda_{em} = 596$ nm) for $LaSiO_2N$:0.06Eu samples (1500 °C, 1525°C, and 1550 °C) and normalized PL spectra ($\lambda_{ex} = 365$ nm) for $LaSiO_2N$:0.06Eu sample.** The inset shows the magnified Fit Peaks 1 of $LaSiO_2N$:0.06Eu samples.

electronegativity than that of $Eu^{3+}$ ions, the Eu–O bond strength became weaker with increasing concentration of $Eu^{2+}$, resulting in weakening of bond strength. Hence the $Eu^{3+}$-$O^{2-}$ bond length became longer. As reported by Lin *et al.*[40], the longer the Eu-O bond, the shorter the energy difference between the 4f and O 2p electrons, and the lower energy position of the CTB.

Additionally, the coordination number of $Eu^{2+}$ was reduced because the $V_o$ increased with an increase of the $Eu^{2+}$ content in the host, which caused the formation of a centroid of the 5d state at a lower level. Thus, as shown in Fig. 8, the 5d excitation band (fit peak 2 and 3) red shifted and the overlapping between PLE of 596 nm and PL enlarged, indicating that the energy transfer ratio between $Eu^{2+}$ and the $^5D_0$ level of $Eu^{3+}$ was enhanced. The energy transfer mode between $Eu^{2+}$ and $Eu^{3+}$ in $LaSiO_2N$: Eu was proposed in Fig. 9. Under the NUV light excitation, $Eu^{2+}$ was excited from the ground state $4f^7(^8S7/2)$ to the excited state $4f^65d^1$. Partial energy relaxed to the ground state through the inherent transition of $Eu^{2+}$, generating a yellow light emission; the rest of energy transferred to the nearest level $^5D_0$ of $Eu^{3+}$, and then 597 nm, 617 nm, 660 nm and 707 nm emissions appeared by a transition to the $^7F_j$ (J = 1, 2, 3 and 4) ground state. With the increase of the preparation temperature, the depressed 5d level showed more overlapping with the $^5D_0$ of $Eu^{3+}$, resulting in the enhancement of the energy transfer between the $Eu^{2+}$ and $Eu^{3+}$ [25]. The increased emission peak position from 550 nm at 1500 °C to 565 nm at 1550 °C and FWHM of emission peak from 116 nm at 1500 °C to 120 nm at 1550 °C also verified the redshift of 5d level[25,26]. The decay curves of $LaSiO_2N$:0.06Eu prepared at different temperatures monitored at 565 nm were depicted in Fig. 10. All decay curves also could be well fitted via the second-order exponential equation and the lifetimes were estimated 1.58, 1.23, and 0.96 μs for $LaSiO_2N$:0.06Eu prepared at 1500 °C, 1525 °C, and 1550 °C, respectively, demonstrating the existence of energy transfer. Consequently, via the increase of preparation temperature, the holistic emission intensity was enhanced owe to the increased crystallinity and reduction process. The relative emission intensity of $Eu^{3+}$ was also increased due to the enhancement of the energy transfer. As a result, the red region of yellow emitting $LaSiO_2N$: Eu phosphor was successfully enhanced.

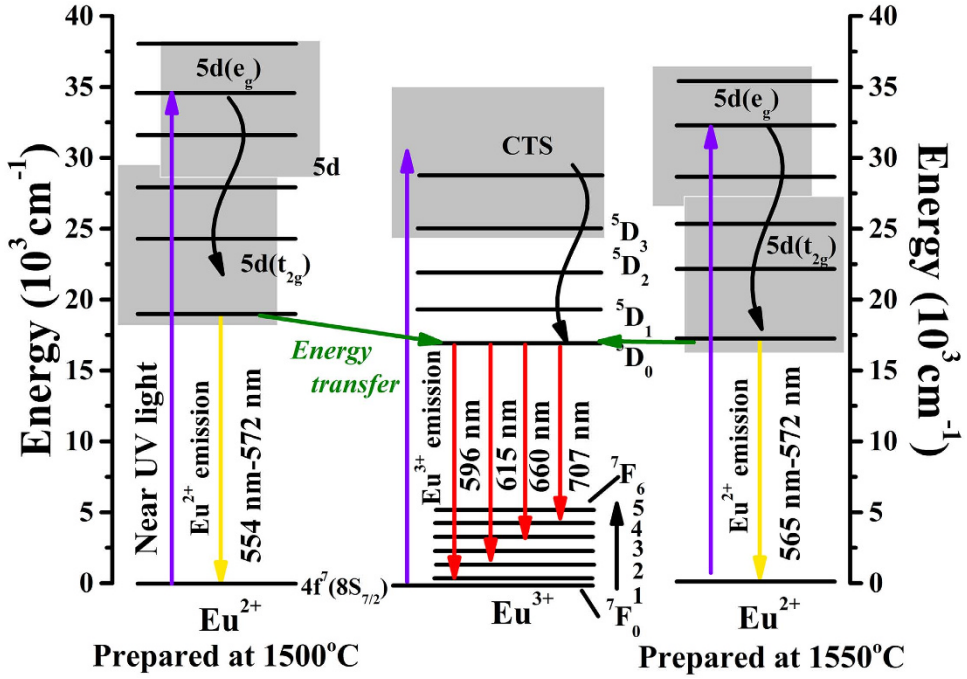


**Figure 9. Schematic of energy transfer in $LaSiO_2N$:0.06Eu.**

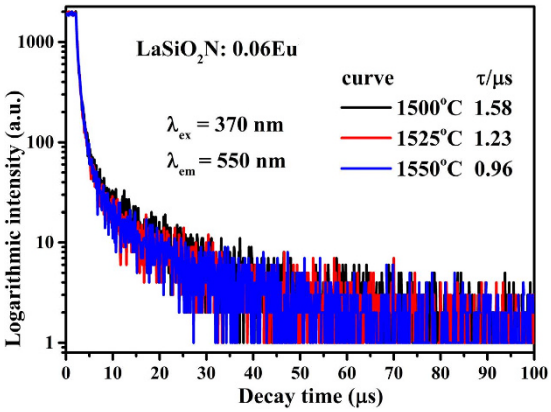


**Figure 10. The decay curves of $LaSiO_2N$:0.06Eu prepared at 1500 °C, 1525 °C, and 1550 °C, respectively.**

The quantum efficiency of phosphors, which is an important technological parameter for practical application, were also been compared. The internal quantum efficiencies (IQE) of $LaSiO_2N$:0.06Eu prepared at different temperature were measured and calculated by the following equations[41]:

$$\eta_{QE} = \frac{\int L_S}{\int E_R + \int E_S} \quad (3)$$

where $L_S$ represents the luminescence emission spectrum of the sample; $E_R$ is the spectrum of the excitation light from the empty integrated sphere (without the sample); $E_S$ means the excitation spectrum for exciting the sample. As given in Figure S2, the IQE of the $LaSiO_2N$:0.06Eu prepared at 1500 °C, 1525 °C and 1550 °C were estimated to be about 3.48%, 12.48% and 20.01%, respectively, under 365 nm excitation. The enhanced IQE matched well with the variation trend of emission intensity. Although the IQE of $LaSiO_2N$:0.06Eu is lower than that of commercial YAG (61%)[42], it can be further improved by optimization of the preparation conditions, because the QE depends closely on the prepared conditions, crystalline defects, particle size and morphology of the phosphor[43,44].

In order to well understand the luminescent performance of this phosphor, the temperature-dependent luminescent properties of $LaSiO_2N$: 0.06Eu phosphor was measured during the temperature ranges of 25–200 °C. As presented in Fig. 11a, the emission intensity decreased with increasing temperature. At 100 °C and 150 °C, the PL intensity quenched to 62.8% and 42.3%. The thermal quenching effect of this phosphor is more intense than

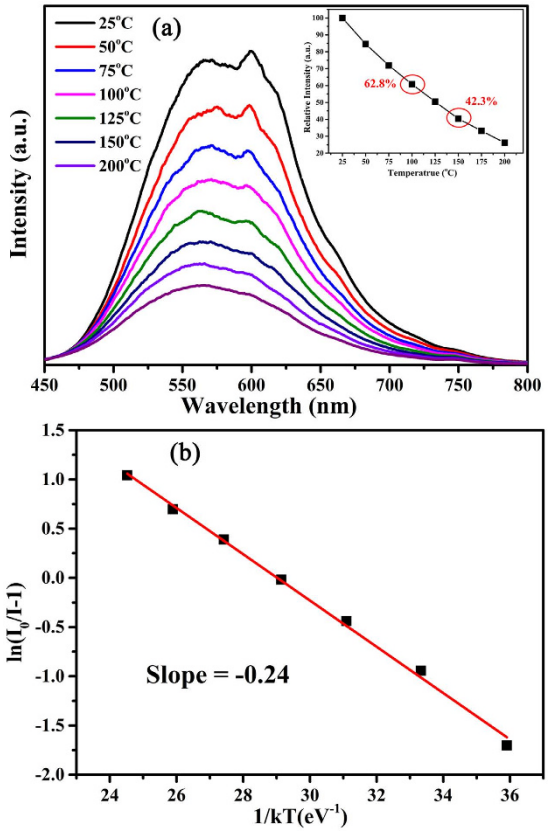


**Figure 11.** (**a**) Temperature-dependent PL spectra ($\lambda_{em} = 365$ nm) and (**b**) the plot of ln (I0/I) vs. 1/T of $LaSiO_2N$:0.06Eu phosphors. The inset shows the emission intensity versus temperature.

the commercial YAG:$Ce^{3+}$ [45], while similar to La–Si–O–N system phosphors[12]. The thermal quenching can be explained by the model of thermal excitation of the 5*d* electron to conduction band states[46,47]. When $Eu^{2+}$ substituted in a trivalent site, the $Eu^{2+}$ had the trend to be ionized to $Eu^{3+}$, which reduced the activation energy and lead to stronger thermal quenching. To determine the activation energy for thermal quenching, the Arrhenius equation was used to estimate the thermal quenching[48]:

$$\ln\left(\frac{I_0}{I}\right) = \ln A - \frac{\Delta E}{kT} \tag{4}$$

where $I_0$ and $I$ mean the luminescence intensity of $LaSiO_2N$:Eu at room temperature and a given temperature, respectively; A is a constant; k presents the Boltzmann constant ($8.617 \times 10^{-5}$ eV $K^{-1}$). Figure 11b plots ln[(I0/I)-1] variation dependence of 1/(kT), and the $\Delta E$ was calculated to be about 0.24 eV.

To further assess the potential application of the $LaSiO_2N$: Eu phosphors, the yellow emitting $LaSiO_2N$:0.01Eu phosphor prepared at 1500 °C and $LaSiO_2N$:0.06Eu phosphors prepared at 1550 °C were mixed with blue-emitting BAM: $Eu^{2+}$ phosphor, respectively, and then the mixtures were severally combined with a 385 nm NUV chip to fabricate white LED lamps. The electroluminescent (EL) spectra of these lamps driven by 30 mA current were depicted in Fig. 12. The CIE color coordinates, CCT and CRI of the fabricated W-LED lamp with $LaSiO_2N$:0.01Eu phosphor prepared at 1500 °C were determined to be (0.32, 0.38), 5959 and 76, respectively (Figure S3 and Fig. 12a). Via utilizing the redshift, varied valence and efficient energy transfer, the fabricated W-LED lamp with the red region enhanced yellow-emitting $LaSiO_2N$:0.06Eu phosphor displayed an entire white spectrum with a CIE color coordinates of (0.33, 0.36), a CCT of 5783 K and a CRI of 87 (Figure S3 and Fig. 12b). Compared with the W-LED lamp using commercial YAG:Ce phosphor in previous study (CIE = 0.302, 0.315; CCT = 7272 K, Ra = 78.38)[3], the CCT of as-fabricated LEDs was relative low and the Ra was high, suggesting that the high CRI warm W-LEDs could be easily obtained by altering the concentration of doping ions and the preparation temperature.

## Conclusions

In summary, a novel Eu-activated $LaSiO_2N$ yellow-emitting phosphor has been synthesized and evaluated for the application in W-LEDs. With the aid of crystal structure, valence-varied, redshift, and energy transfer, the red region enhanced yellow-emitting $LaSiO_2N$: Eu phosphor has been designed and realized by controlling the concentration of doping ions and the preparation temperature. A high CRI and warm W-LED lamp was obtained in combination with this phosphor, proving that the red region enhanced $LaSiO_2N$: Eu phosphor has a great

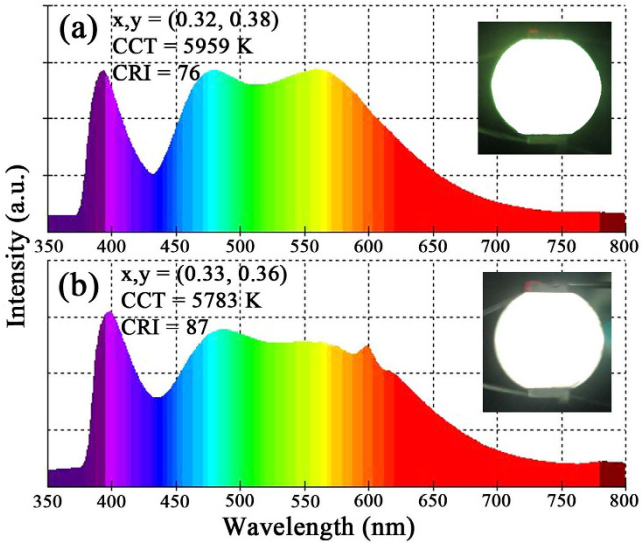


**Figure 12.** Electroluminescence spectra of W-LED lamps fabricated using a 385 nm NUV chip in combination with the mixed phosphors consisting of blue-emitting BAM:$Eu^{2+}$ phosphor and yellow-emitting (**a**) $LaSiO_2N$:0.01Eu phosphor prepared at 1500 °C, (**b**) $LaSiO_2N$:0.06Eu phosphor prepared at 1550 °C. Insets show the digital images of the LED package with an input of 30 mA current.

potential for the application in W-LEDs. More importantly, this study would provide a new strategy for designing Eu-activated yellow-emitting phosphors by synergistically enhancing the red region and emission intensity to adjust the CCT and CRI for warm W-LEDs application without reducing the other luminescence properties.

## Methods

**Materials and Synthesis.** The $LaSiO_2N$:Eu was synthesized from stoichiometric mixtures of $La_2O_3$ (analytical reagent (A. R.)), α-Si3N4 (A. R.) and $Eu_2O_3$ (A. R.). The ground powders were placed in alumina crucibles and fired for 6 h in a reducing atmosphere (10% $H_2$ + 90% $N_2$) at 1500 °C, 1525 °C and 1550 °C, respectively. Then, the precursor was reground and heated again at same condition. Thereafter, the samples were cooled down to room temperature naturally and powdered for subsequent analysis.

**Materials Characterization.** Powder X-ray diffraction on a D8 Advance diffractometer (Germany) with graphite-monochromatized Cu Kα radiation (λ = 0.154 06 nm) was recorded for the structure of all samples. Photoluminescence spectra were collected using a Hitachi F-4600 fluorescence spectrophotometer (Japan) equipped with a 150 W Xe lamp as the excitation source. Diffuse reflection spectra were recorded using a Shimadzu UV-3600 UV−vis−NIR spectrophotometer attached with an integrating sphere. BaSO4 was used as a reference for 100% reflectance. The morphology was observed using scanning electron microscopy (SEM; JSM-6460LV, JEOL, Japan). X-ray photoelectron spectroscopy (XPS) measurements were performed in a PHI 5300 ESCA system using an Al Ka X-ray source with constant pass energy of 55.00 eV. The charge effect referred to the C1s signal (284.6 eV). The room-temperature luminescence decay curves were obtained from a spectrofluorometer (Horiba, Jobin Yvon TBXPS) using a tunable pulse laser radiation (nano-LED) as the excitation. Quantum efficiency was measured by a fluoromax-4 spectrofluorometer (Horiba, Jobin Yvon) with an integral sphere at room temperature.

## References

1. Lu, W., Jia, Y., Zhao, Q., Lv, W. & You, H. Design of a luminescence pattern via altering the crystal structure and doping ions to create warm white LEDs. *Chem. Commun.* **50,** 2635–2637 (2014).
2. Pust, P. *et al.* Ca [$LiAl_3N_4$]: $Eu^{2+}$ A Narrow-Band Red-Emitting Nitridolithoaluminate. *Chem. Mater.* **26,** 3544–3549 (2014).
3. Yeh, C.-W. *et al.* Origin of Thermal Degradation of $Sr_{2-x}Si_5N_8$:$Eu_x$ Phosphors in Air for Light-Emitting Diodes. *J. Am. Chem. Soc.* **134,** 14108–14117 (2012).
4. Huang, C.-H., Chiu, Y.-C., Yeh, Y.-T., Chan, T.-S. & Chen, T.-M. $Eu^{2+}$-Activated $Sr_8ZnSc(PO_4)_7$: A Novel Near-Ultraviolet Converting Yellow-Emitting Phosphor for White Light-Emitting Diodes. *ACS. Appl. Mater. Inter.* **4,** 6661–6668 (2012).
5. Shang, M., Li, C. & Lin, J. How to produce white light in a single-phase host? *Chem. Soc. Rev.* **43,** 1372–1386 (2014).
6. Zhang, X., Fei, L., Shi, J. & Gong, M. $Eu^{2+}$-activated $Ba_2Mg(BO_3)_2$ yellow-emitting phosphors for near ultraviolet-based light-emitting diodes. *Physica B: Condensed Matter* **406,** 2616–2620 (2011).
7. Wu, Z., Gong, M., Shi, J., Wang, G. & Su, Q. Dibarium magnesium diphosphate yellow phosphor applied in InGaN-based LEDs. *Chem. Lett.* **36,** 410–411 (2007).
8. Jang, H. S., Kim, H. Y., Kim, Y.-S., Lee, H. M. & Jeon, D. Y. Yellow-emitting γ-$Ca_2SiO_4$: $Ce^{3+}$, $Li^+$ phosphor for solid-state lighting: luminescent properties, electronic structure, and white light-emitting diode application. *Opt. Express.* **20,** 2761–2771 (2012).
9. Song, W.-S., Kim, Y.-S. & Yang, H. Yellow-emitting phosphor of $Sr_3B_2O_6$:$Eu^{2+}$ for application to white light-emitting diodes. *Mater. Chem. Phys.* 117, 500–503 (2009).
10. Jang, H. S. & Jeon, D. Y. White light emission from blue and near ultraviolet light-emitting diodes precoated with a $Sr_3SiO_5$: $Ce^{3+}$, $Li^+$ phosphor. *Opt. Lett.* **32,** 3444–3446 (2007).

11. Wu, Y.-C., Chen, T.-M., Chiu, C.-H. & Mo, C.-N. Luminescence and Spectroscopic Properties of Yellow-Emitting Carbonitride Phosphors and Their Application in White LEDs. *J. Electrochem. Soc.* **157,** J342–J346 (2010).
12. Dierre, B., Xie, R.-J., Hirosaki, N. & Sekiguchi, T. Blue emission of $Ce^{3+}$ in lanthanide silicon oxynitride phosphors. *J. Mater. Res.* **22,** 1933–1941 (2007).
13. Kim, B.-H., Kang, E.-H., Choi, S.-W. & Hong, S.-H. Luminescence properties of $La_2Si_6O_3N_8$:$Eu^{2+}$ phosphors prepared by spark plasma sintering. *Opt. Mater.* **36,** 182–185 (2013).
14. Xie, R.-J. & Hirosaki, N. Silicon-based oxynitride and nitride phosphors for white LEDs—A review. *Sci. Technol. Adv. Mat.* **8,** 588–600 (2007).
15. Li, G., Tian, Y., Zhao, Y. & Lin, J. Recent progress in luminescence tuning of $Ce^{3+}$ and $Eu^{2+}$-activated phosphors for pc-WLEDs. *Chem. Soc. Rev.* **44,** 8688–8713 (2015).
16. Hu, L. *et al.* Luminescence of $Ce^{3+}$ in lanthanum silicon oxynitride. *Chinese. Phys. B.* **19,** 127807 (2010).
17. Dorenbos, P. Energy of the first $4f^7 \rightarrow 4f^6 5d$ transition of $Eu^{2+}$ in inorganic compounds. *J. Lumin.* **104,** 239–260 (2003).
18. Van Krevel, J. W. H., Hintzen, H. T., Metselaar, R. & Meijerink, A. Long wavelength $Ce^{3+}$ emission in Y–Si–O–N materials. *J. Alloys Compd.* **268,** 272–277 (1998).
19. Harris, R. K., Leach, M. J. & Thompson, D. P. Nitrogen-15 and oxygen-17 NMR spectroscopy of silicates and nitrogen ceramics. *Chem. Mater.* **4,** 260–267 (1992).
20. Liu, H., Luo, Y., Mao, Z., Liao, L. & Xia, Z. A novel single-composition trichromatic white-emitting $Sr_{3.5}Y_{6.5}O_2(PO_4)_{1.5}(SiO_4)_{4.5}$: $Ce^{3+}$/$Tb^{3+}$/$Mn^{2+}$ phosphor: synthesis, luminescent properties and applications for white LEDs. *J. Mater. Chem. C.* **2,** 1619–1627 (2014).
21. Zhang, N., Guo, C., Zheng, J., Su, X. & Zhao, J. Synthesis, electronic structures and luminescent properties of $Eu^{3+}$ doped $KGdTiO_4$. *J. Mater. Chem. C.* **2,** 3988–3994 (2014).
22. Im, W. B. *et al.* $Sr_{2.975-x}Ba_xCe_{0.025}AlO_4F$: a Highly Efficient Green-Emitting Oxyfluoride Phosphor for Solid State White Lighting. *Chem. Mater.* **22,** 2842–2849 (2010).
23. Zhang, X. *et al.* Tunable Luminescent Properties and Concentration-Dependent, Site-Preferable Distribution of $Eu^{2+}$ Ions in Silicate Glass for White LEDs Applications. *ACS. Appl. Mater. Inter.* **7,** 10044–10054 (2015).
24. Chen, J. *et al.* The luminescence properties of novel $\alpha$-$Mg_2Al_4Si_5O_{18}$:$Eu^{2+}$ phosphor prepared in air. *RSC Adv.* **4,** 18234–18239 (2014).
25. Mao, Z.-y. & Wang, D.-j. Color Tuning of Direct White Light of Lanthanum Aluminate with Mixed-Valence Europium. *Inorg. Chem.* **49,** 4922–4927 (2010).
26. Chen, J. *et al.* Emission red shift and energy transfer behavior of color-tunable $KMg_4(PO_4)_3$:$Eu^{2+}$,$Mn^{2+}$ phosphors. *J. Mater. Chem. C.* **3,** 5516–5523 (2015).
27. Yang, W.-J., Luo, L., Chen, T.-M. & Wang, N.-S. Luminescence and energy transfer of Eu-and Mn-coactivated $CaAl_2Si_2O_8$ as a potential phosphor for white-light UVLED. *Chem. Mater.* **17,** 3883–3888 (2005).
28. Grabmaier, B. *Luminescent materials*. (Springer Verlag, 1994).
29. Xia, Z., Zhou, J. & Mao, Z. Near UV-pumped green-emitting $Na_3(Y,Sc)Si_3O_9$:$Eu^{2+}$ phosphor for white-emitting diodes. *J. Mater. Chem. C.* **1,** 5917–5924 (2013).
30. Chen, J. *et al.* Crystal structure and Temperature-Dependent Luminescence Characteristics of $KMg_4(PO_4)_3$:$Eu^{2+}$ phosphor for White Light-emitting diodes. *Sci. Rep.* **5,** 9673 (2015).
31. Tran, N. T., You, J. P. & Shi, F. G. Effect of phosphor particle size on luminous efficacy of phosphor-converted white LED. *J. Lightwave Technol.* **27,** 5145–5150 (2009).
32. Lin, C. C. & Liu, R.-S. Advances in Phosphors for Light-emitting Diodes. *J. Phys. Chem. Lett.* **2,** 1268–1277 (2011).
33. Chen, J., Liu, Y. & Fang, M. & Huang, Z. Luminescence Properties and Energy Transfer of Eu/Mn-Coactivated $Mg_2Al_4Si_5O_{18}$ as a Potential Phosphor for White-Light LEDs. *Inorg. Chem.* **53,** 11396–11403 (2014).
34. Wang, K. & Reeber, R. Thermal defects and thermal expansion of ionic crystals at high temperatures. *physica status solidi (a)* **146,** 621–627 (1994).
35. Schaefer, H.-E., Frenner, K. & Würschum, R. High-temperature atomic defect properties and diffusion processes in intermetallic compounds. *Intermetallics* **7,** 277–287 (1999).
36. Jeong, J. H. *et al.* Li doping effect on the luminescent characteristics of $YVO_4$:$Eu^{3+}$ thin films grown by pulsed laser deposition. *Appl. Surf. Sci.* **253,** 8273–8277 (2007).
37. Yi, S.-s. *et al.* Enhanced luminescence of $Gd_2O_3$: $Eu^{3+}$ thin-film phosphors by Li doping. *Appl. Phys. Lett.* **84** (2004).
38. Balakrishnaiah, R. *et al.* Enhanced luminescence properties of $YBO_3$: $Eu^{3+}$ phosphors by Li-doping. *Mater. Res. Bull.* **46,** 621–626 (2011).
39. Garcia-Hipolito, M., Martinez, E., Alvarez-Fregoso, O., Falcony, C. & Aguilar-Frutis, M. A. Preparation and characterization of Eu doped zirconia luminescent films synthesized by the pyrosol technique. *J. Mater. Sci. Lett.* **20,** 1799–1801 (2001).
40. Lin, J., You, L., Lu, G., Yang, L. & Su, M. Structural and luminescent properties of $Eu^{3+}$ doped $Gd_{17.33}(BO_3)_4(B_2O_5)_2O_{16}$. *J. Mater. Chem.* **8,** 1051–1054 (1998).
41. Xu, Y. *et al.* Efficient near-infrared down-conversion in $Pr^{3+}$–$Yb^{3+}$ codoped glasses and glass ceramics containing $LaF_3$ nanocrystals. *J. Phys. Chem. C.* **115,** 13056–13062 (2011).
42. Haranath, D., Chander, H., Sharma, P. & Singh, S. Enhanced luminescence of $Y_3Al_5O_{12}$:$Ce^{3+}$ nanophosphor for white light-emitting diodes. *Appl. Phys. Lett* **89,** 173118 (2006).
43. Dexter, D. & Schulman, J. H. Theory of concentration quenching in inorganic phosphors. *J. Chem. Phys.* **22,** 1063–1070 (1954).
44. Bachmann, V., Ronda, C., Oeckler, O., Schnick, W. & Meijerink, A. Color point tuning for (Sr, Ca, Ba)$Si_2O_2N_2$: $Eu^{2+}$ for white light LEDs. *Chem. Mater.* **21,** 316–325 (2008).
45. Shao, Q., Dong, Y., Jiang, J., Liang, C. & He, J. Temperature-dependent photoluminescence properties of (Y, Lu)$_3Al_5O_{12}$: $Ce^{3+}$ phosphors for white LEDs applications. *J. Lumin.* **131,** 1013–1015 (2011).
46. Happek, U., Basun, S., Choi, J., Krebs, J. & Raukas, M. Electron transfer processes in rare earth doped insulators. *J. Alloys Compd.* **303,** 198–206 (2000).
47. Dorenbos, P. Thermal quenching of $Eu^{2+}$ 5d–4f luminescence in inorganic compounds. *J. Phys.: Condens. Matter* **17,** 8103 (2005).
48. Geng, D., Lian, H., Shang, M., Zhang, Y. & Lin, J. Oxonitridosilicate $Y_{10}$ ($Si_6O_{22}N_2$) $O_2$: $Ce^{3+}$, $Mn^{2+}$ phosphors: a facile synthesis via the soft-chemical ammonolysis process, luminescence, and energy-transfer properties. *Inorg. Chem.* **53,** 2230–2239 (2014).


## Acknowledgements

The authors gratefully thank the financial support of the National Natural Science Foundation of China (No. 51472223), the Program for New Century Excellent Talents in University of Ministry of Education of China (No. CET-12-0951) and the Fundamental Research Funds for the Central Universities (No. 2652015020).

## Author Contributions

Y.L. and J.C. conceived the project. J.C. and L.M. designed and performed the experiments. J.C., P.P. and H.L. analyzed the data. J.C. and Q.C. wrote the manuscript. All the authors discussed the results and commented on the manuscript at all stages.

## Additional Information

**Supplementary information** accompanies this paper at http://www.nature.com/srep

**Competing financial interests:** The authors declare no competing financial interests.

**How to cite this article**: Chen, J. *et al.* Design of a Yellow-Emitting Phosphor with Enhanced Red Emission via Valence State-control for Warm White LEDs Application. *Sci. Rep.* **6**, 31199; doi: 10.1038/srep31199 (2016).